Noise sustained pattern growth: Bulk versus boundary effects

M. Lücke
Institut für Theoretische Physik, Universität des Saarlandes, D-66041 Saarbrücken, Germany

A. Szprynger
Institute of Low Temperature and Structure Research, Polish Academy of Sciences, 50-950 Wrocław 2, Post Office Box 937, Poland

(Received 31 October 1996)

The effect of thermally generated bulk stochastic forces on the statistical growth dynamics of forward bifurcating propagating macroscopic patterns is compared with the influence of fluctuations at the boundary of a semi-infinite system, $0<x$. To that end the linear complex Ginzburg-Landau amplitude equation with additive stochastic forcing is solved by a spatial Laplace transformation in the presence of arbitrary boundary conditions for the fluctuations of the pattern amplitude at $x=0$. A situation where the latter are advected with an imposed through-flow from an outside upstream part towards the inlet boundary at $x=0$ is investigated in more detail. The spatiotemporal growth behavior in the convectively unstable regime is compared with recent work by J. B. Swift, K. L. Babcock, and P. C. Hohenberg [Physica A **204**, 625 (1994)] where a special boundary condition is imposed. [S1063-651X(97)02905-X]

PACS number(s): 47.20.−k, 43.50.+y, 47.60.+i, 05.40.+j

I. INTRODUCTION

Nonequilibrium extended systems that undergo a pattern forming instability with nonzero group velocity [1]—whether the latter arises in open-flow configurations [2,3] via an imposed through-flow [4–15] or internally from a bifurcation to traveling waves [16–18]—show a peculiar sensitivity to perturbations in the so-called convectively unstable parameter regime [19,20]. Therein initially spatially localized perturbations superimposed on some basic unstable, macroscopically unstructured nonequilibrium state of the system are advected downstream by the group velocity. Simultaneously they are selectively amplified [20,21] according to the deterministic amplification mechanism that occurs near the pattern forming bifurcation [1]. Thus, advection spatially deconvolutes the pattern growth from its cause—the perturbation source. But the latter leaves its signature via the bifurcation-induced, deterministic amplification process on the spatiotemporal properties of the downstream growing macroscopic nonequilibrium structures. The statistical dynamics of fluctuations of these structures is easily detectable [5–8,10–12,17,18], thus providing information about the small perturbations that have triggered their growth.

The feasibility to distinguish the influence of different perturbation sources—e.g., those that are external to the system under study versus internal thermal noise—on the macroscopic pattern growth in a very direct way has attracted much research activity recently [6–8,10–12,17,18]. Here one has to keep in mind that the deterministic bifurcation dynamics of the macroscopic structure forming instability determines which of the modes that a perturbation source emits is amplified and which one decays in the downstream direction. And as long as the mode amplitudes are still small each of the perturbation modes evolves separately and independently: the bifurcation dynamics is initially linear with saturating nonlinearities being irrelevant, thus producing exponential growth with time and downstream distance.

Hence, in a system with group velocity in the positive x direction one expects that fluctuations generated near the inlet boundary at $x=0$ and/or perturbations that might enter the system via the inlet are most important. They have the longest advection or amplification time to grow in the flow before they reach a particular observation point at a downstream location $x>0$. Therefore a careful analysis of the influence of the inlet boundary condition relative to the effect of bulk (fluctuating) forces is necessary, particularly in view of the fact that both sources cause exponential growth. Such an analysis should be able to shed some light on the problem of whether in bounded experimental systems it is internal bulk generated thermal noise that triggers and sustains the growth of macroscopic vortex structures in the convectively unstable regime or another kind of environment-produced perturbation that might, e.g., be advected from the inlet boundary into the bulk.

On the theoretical side the effect of noise on the pattern forming process has been investigated mainly within the framework of the complex Ginzburg-Landau amplitude equation (CGLE). It describes the slow spatiotemporal behavior of the complex amplitude $A(x,t)$ of the critical mode of the pattern that can grow first when crossing the bifurcation threshold. Bulk thermal noise is incorporated in this approximation scheme by fluctuating volume forces $f(x,t)$ that act additively on $A(x,t)$ and that are derived [22–26] for local thermal equilibrium conditions of driven systems from the linear Landau-Lifshitz equations of fluctuating hydrodynamics around global thermal equilibrium [27]. The problem of the inlet boundary condition that arises with the CGLE in a finite domain has been addressed only in some idealized way: Deissler [28] imposes $A=0$ at the inlet. Lücke and Recktenwald [29] investigate the pattern growth resulting from an inlet boundary condition that is produced by thermal equilibrium transverse momentum fluctuations that are advected into the system at $x=0$. Babcock, Ahlers, and Cannell [8] have solved the stochastic CGLE numerically in a system that was augmented in the upstream direction, i.e., to negative x by a small subcritical part and compared with

imposing $A=0$ at $x=0$. Swift, Babcock, and Hohenberg (SBH) [25] consider solutions of the stochastic CGLE where the amplitude fluctuations $A(x=0,t)$ at the boundary are strongly correlated with the bulk thermal forcing f.

In this paper we first of all solve the stochastic CGLE subject to arbitrary inlet boundary conditions with a spatial Laplace transformation method. We investigate the influence of thermally generated bulk additive forcing on the statistical dynamics of downstream growing amplitude fluctuations in comparison with the effect of statistically stationary inlet fluctuations that are independent of the bulk forcing. Furthermore, we use a simple model to estimate fluctuations that are swept with an imposed through-flow into some experimental systems via the inlet. This allows us to assess more quantitatively the importance of such inlet fluctuations relative to bulk thermal forcing. Experimental setups to tune and control the former are briefly discussed as well. Finally we compare our results in detail with the results of SBH.

Our paper is organized as follows: In Sec. II the linear stochastic CGLE with thermally generated bulk additive forcing is briefly reviewed. The solution for the fluctuating amplitudes in frequency space, $A(x,\omega)$, and their correlation spectra are given in Sec. III. Section IV presents the model for inlet fluctuations and compares their downstream evolution with the growth of bulk generated fluctuations. Section V contains a summary. In Appendix A we present the ''space-retarded, causal'' Green function of our solution in the convectively unstable regime. In Appendix B we compare our results for the Green function, amplitude fluctuations, and correlation spectra with those of SBH.

II. SYSTEMS

The systems that we have in mind show a continuous, i.e., hysteresis-free, transition, say, from a spatially homogeneous state to a spatially structured one. Thus, a spatially periodic solution branches in a forward bifurcation out of the basic solution at a critical control parameter. The most intensively studied examples for such systems are the Rayleigh-Bénard (RB) problem of straight roll convection vortices in a fluid layer heated from below [1] or the rotating Taylor-Couette (TC) problem of axisymmetric toroidal Taylor vortices in the annulus between concentric cylinders of which the inner one is rotating [1,30]. But our investigation, being based on the CGLE for such one-dimensional (1D) patterns, also includes other problems for which this equation captures the essential parts of the pattern formation process. Nevertheless, we shall use in the remainder of this paper the terminology of the RB or TC system. Thus, we consider in particular open RB (TC) setups with an externally imposed horizontal (axial) mean flow through a not too wide rectangular convective channel (annulus between concentric cylinders). Then the deterministic field equations show an oscillatory instability. The structureless, stationary basic flow without vortices is stable for Rayleigh numbers Ra (Taylor numbers T) below a critical threshold $\mathrm{Ra}_c(\mathrm{Re})$ [$T_c(\mathrm{Re})$] that depends on the through-flow Reynolds number Re. At the critical threshold a stable, spatially extended, temporally oscillatory state of downstream propagating vortices branches off the basic state. The latter is unstable and the former is stable for supercritical driving.

We use the relative control parameter

$$\mu=\frac{\mathrm{Ra}}{\mathrm{Ra}_c(\mathrm{Re})}-1 \quad \text{or} \quad \mu=\frac{T}{T_c(\mathrm{Re})}-1 \tag{2.1}$$

to measure the distance from the onset of propagating vortex flow for $\mathrm{Re}\neq 0$ and of stationary vortex flow for $\mathrm{Re}=0$, respectively. In this notation $\mu_c=0$, i.e.,

$$\epsilon_c(\mathrm{Re})=\frac{\mathrm{Ra}_c(\mathrm{Re})}{\mathrm{Ra}_c(\mathrm{Re}=0)}-1 \quad \text{or} \quad \epsilon_c(\mathrm{Re})=\frac{T_c(\mathrm{Re})}{T_c(\mathrm{Re}=0)}-1 \tag{2.2}$$

is the critical reduced threshold for the onset of propagating vortex flow. The shear forces of the through-flow slightly stabilize the homogeneous basic state, so $\epsilon_c(\mathrm{Re})$ slightly increases with Re [2,4,6–8,31]. Note that in the RB system we consider so-called transverse vortices whose roll axes are enforced to lie perpendicular to the through-flow direction by the geometrical design of the rectangular convection channel. So for not too large Re the critical wave vector of the vortex patterns is oriented in both cases along the x direction of the through-flow, $\mathbf{k}_c=k_c\mathbf{e}_x$.

A. Amplitude equation approximation

For small supercritical control parameters, $0<\mu\ll 1$, the macroscopic vortex dynamics is governed by a narrow band of near critical modes. This allows one to represent the hydrodynamic fields within an amplitude equation approximation [1] by a complex amplitude $A(x,t)$ multiplying the critical mode

$$w(x,\mathbf{r}_\perp;t)=A(x,t)e^{i(k_c x-\omega_c t)}\hat{w}(\mathbf{r}_\perp)+\text{c.c.} \tag{2.3}$$

Here w is, for example, a component of the vortex velocity field. The critical wave number k_c, frequency ω_c [4,6–8,31–33], and eigenfunction $\hat{w}(\mathbf{r}_\perp)$ [32,34] depending on the coordinates $\mathbf{r}_\perp$ perpendicular to the critical wave vector of the downstream propagating vortex structures are known as functions of Re from a linear stability analysis of the basic flow.

In the absence of fluctuations the spatiotemporal behavior of the complex vortex amplitude $A(x,t)$ is determined by the 1D CGLE:

$$\tau_0(\partial_t+v\partial_x)A(x,t)=[(1+ic_0)\mu+(1+ic_1)\xi_0^2\partial_x^2]A(x,t)+(\text{nonlinear terms}). \tag{2.4}$$

The coefficients τ_0 and ξ_0^2 are even in Re while the group velocity v and the imaginary parts c_0,c_1 are odd in Re [5,31].

B. Absolute and convective instability

For small μ and Re the control parameter plane is divided into three domains characterized by different growth behavior of *linear* perturbations of the basic flow state. In the presence of through-flow one has to distinguish [19] between the spatiotemporal growth behavior of spatially localized perturbations and that of spatially extended ones. Below the threshold $\mu=0$ for onset of propagating vortex patterns any

perturbation, spatially localized as well as extended, decays. This is the parameter regime of absolute stability of the basic state.

For $\mu>0$ extended perturbations can grow. However, a spatially localized perturbation, i.e., a packet of plane wave perturbations, is advected in the so-called convectively unstable parameter regime faster downstream than it grows—while growing in the comoving frame it moves out of the system [19–21,35]. Thus, the downstream as well as the upstream facing intensity front of the vortex packet move in the same direction, namely, downstream. A spatially localized perturbation is blown out of any system of finite length and the basic state is reestablished. It therefore requires a persistent source of perturbations such as, e.g., noise operating in the bulk or fluctuations entering the system via the inlet to sustain a vortex pattern in the convectively unstable regime [21]. The spatiotemporal behavior of such ''noise sustained structures'' [8,12] being determined by the noise source thus allows one to infer properties of the latter from the former.

In the absolutely unstable regime a localized perturbation not only grows in the downstream direction but it grows and spatially expands also in the upstream direction until the upstream propagating front encounters the inlet in a finite system [13]. The final nonlinear stucture [4,5,9,10,13–15,36] resulting in such a situation is self-sustained and stable. For sufficiently large amplitudes this structure is dominated by the deterministic contributions in the relevant balance equations and thus it is insensitive to, say, thermal noise.

Within the framework of the amplitude equation the boundary between absolute and convective instability is given by [21]

$$\mu^c_{\mathrm{conv}}=\frac{\tau_0^2 v^2}{4(1+c_1^2)\xi_0^2}. \tag{2.5}$$

Thus, the convectively unstable regime investigated here is characterized by $0<\mu<\mu^c_{\mathrm{conv}}$ or, equivalently, by the reduced group velocity

$$V=\frac{\tau_0}{\xi_0\sqrt{(1+c_1^2)\mu}}v=2\sqrt{\frac{\mu^c_{\mathrm{conv}}}{\mu}}, \tag{2.6}$$

being larger than 2. It should be mentioned that the amplitude equation approximation (2.5) of μ^c_{conv} describes the boundary between absolute and convective instability resulting from the full hydrodynamic field equations [8,37] very well in the RB and TC systems for the small Reynolds numbers considered here.

C. Stochastic amplitude equation

The starting point of most theoretical approaches to describe the effect of thermal noise on macroscopic hydrodynamic pattern growth is the Langevin concept of Landau and Lifshitz [27]. Therein the linear hydrodynamic field equations are heuristically supplemented by Gaussian distributed statistically stationary stochastic forces with zero mean. Their two-point correlation functions reflect the isotropy and translational invariance of an unbounded system and their frequency and wave vector spectra are white. Projection [22–26] of these equations onto the critical modes leads then to the linear stochastic CGLE,

$$[\tau_0(\partial_t+v\partial_x)-(1+ic_0)\mu-(1+ic_1)\xi_0^2\partial_x^2]A(x,t)=f(x,t), \tag{2.7}$$

with Gaussian distributed complex forces $f(x,t)$ that are δ correlated in space and time:

$$\langle f(x,t)\rangle=\langle f(x,t)f(x',t')\rangle=0, \tag{2.8a}$$

$$\langle f(x,t)[f(x',t')]^*\rangle=F\delta(x-x')\delta(t-t'). \tag{2.8b}$$

Here the asterisk implies complex conjugation. The noise strength F has been evaluated by several authors [22–26] for the RB and TC systems without through-flow and with different boundary conditions. Since we do not need the specific values of F we shall not dwell on questions of whether and how the forces are changed by finite-size effects, system geometry, and the through-flow. We rather take Eqs. (2.7) and (2.8) as the starting point for our investigations.

However, for later use we mention that our F is related via $F=2\xi_0\tau_0F_A^{\mathrm{SBH}}$ to the noise strength F_A^{SBH} given in Eqs. (2.10)–(2.16) of SBH. We would also like to mention that the value of F characterizing a particular system depends on the arbitrary choice of the normalization condition for the linear critical mode $\hat{w}(\mathbf{r}_\perp)$ that enters into Eq. (2.3) and that establishes the relation between the physically observable order parameter field $w(x,\mathbf{r}_\perp;t)$ and the complex amplitude A of the critical mode.

III. LINEAR STOCHASTIC CGLE IN SEMI-INFINITE SYSTEMS

In this section we discuss the statistical dynamics of pattern growth in the convectively unstable parameter regime as described by the stochastically forced linear CGLE (2.7). We consider a semi-infinite system with the through-flow entering the system at $x=0$. This flow transports fluctuations into the system that we specify by imposing an inlet boundary condition $A(x=0,t)$ on the amplitude A. We consider situations in which $A(x=0,t)$ is the result of a statistically stationary process; see Sec. IV A for a model. Thus, with the bulk forces $f(x,t)$ being also statistically stationary we restrict our investigations to the long-time statistically stationary fluctuations of $A(x,t)$—initial transients occurring in experiments after, e.g., changing control parameters have died out. Under these circumstances we found it convenient to perform part of our analysis in frequency space. After a temporal Fourier transformation,

$$A(x,\omega)=\int_{-\infty}^{\infty}dt e^{i\omega t}A(x,t), \tag{3.1}$$

the stochastic CGLE becomes an ordinary, second-order, inhomogeneous differential equation

$$[\tau_0(-i\omega+v\partial_x)-(1+ic_0)\mu-(1+ic_1)\xi_0^2\partial_x^2]A(x,\omega)=f(x,\omega), \tag{3.2a}$$

which is to be solved subject to the inlet boundary condition $A(x=0,\omega)$. A condition on the derivative of A at the inlet or,

equivalently, on the behavior of A for $x\to+\infty$ follows from a physical requirement discussed in Sec. III A below.

For later use we rewrite the CGLE in the form

$$-(1+ic_1)\xi_0^2(\partial_x-iK_1)(\partial_x-iK_2)A(x,\omega)=f(x,\omega), \tag{3.2b}$$

which displays the spatial eigenvalues $K_{1,2}$ of the CGLE explicitly—in the solution of Eq. (3.2) there appear contributions of the form e^{iK_1x} and e^{iK_2x}, where $K_{1,2}$ are the complex ω-dependent characteristic exponents, i.e., spatial eigenvalues of Eq. (3.2):

$$\xi_0\sqrt{1+ic_1}K_{1\atop 2}=\pm i\sqrt{(1-ic_1)\mu_{\rm conv}^c-(1+ic_0)\mu-i\omega\tau_0}-i\sqrt{(1-ic_1)\mu_{\rm conv}^c}. \tag{3.3}$$

The physically relevant characteristic exponent that controls the spatial growth of vortices in the downstream direction is K_1, whereas the second eigenvalue of the CGLE is such that $\mathrm{Im}K_2<0$ for all μ and all ω.

$\mathrm{Im}K_1(\omega;\mu)$ is for $\mu<0$ positive so that the spatial growth rate $-\mathrm{Im}K_1$ is negative, implying spatial decay of each frequency mode ω. For $\mu>0$ selective amplification of frequency modes out of a finite band $\omega_-<\omega<\omega_+$ occurs:

$$\mathrm{Im}K_1(\omega;0<\mu<\mu_{\rm conv}^c)<0 \quad \text{for} \quad \omega_-<\omega<\omega_+ \tag{3.4a}$$

$$\mathrm{Im}K_1(\omega;0<\mu<\mu_{\rm conv}^c)>0 \quad \text{for } \omega<\omega_- \quad \text{and} \quad \omega>\omega_+. \tag{3.4b}$$

The band limits for amplification are

$$\tau_0\omega_\pm=\pm 2\sqrt{(1+c_1^2)\mu\mu_{\rm conv}^c}+(c_1-c_0)\mu. \tag{3.5}$$

$\mathrm{Im}K_1$ has a quadratic minimum at the frequency

$$\omega_m=-(c_0+c_1)\mu/\tau_0, \tag{3.6}$$

which is, due to the smallness of c_0 and c_1, in general located close to $\omega=0$. Thus, the frequency mode with largest spatial growth is ω_m.

For plots of $-\mathrm{Im}K_1$ versus ω see, e.g., [29], Fig. 1 and [8], Fig. 14. The relations to our exponent K_1 are $iK_1=\kappa$ [29]$=\beta$ [8].

A. Spatial Laplace transformation

We have solved the CGLE (3.2) with the Green's function method and, equivalently, using a spatial Laplace transformation. The latter method most clearly displays the influence of the inlet boundary properties on the solution. Thus, we start with the latter method here and present the relation to the former in Appendix A.

We use the spatial Laplace transformation

$$A(K)=-i\int_0^\infty dx e^{-iKx}A(x) \quad (K \text{ complex}). \tag{3.7}$$

Here the second argument—ω or t—of A is suppressed. Using the transformation properties

$$\partial_x A(x)\leftrightarrow iKA(K)+iA(x)|_{x=0}, \tag{3.8a}$$

$$\partial_x^2 A(x)\leftrightarrow -K^2A(K)+i(\partial_x+iK)A(x)|_{x=0} \tag{3.8b}$$

the Laplace transformed CGLE (3.2) reads

$$(1+ic_1)\xi_0^2(K-K_1)(K-K_2)A(K,\omega)=i(1+ic_1)\xi_0^2[\partial_x+i(K-K_1-K_2)]A(x,\omega)|_{x=0}+f(K,\omega). \tag{3.9}$$

Its mathematically formal, *physically unrestricted* solution

$$A(K,\omega)=\frac{i[\partial_x+i(K-K_1-K_2)]A(x,\omega)|_{x=0}}{(K-K_1)(K-K_2)}+\frac{f(K,\omega)}{(1+ic_1)\xi_0^2(K-K_1)(K-K_2)} \tag{3.10}$$

contains poles in the complex K plane at K_1 and at K_2.

Now in the *physical* solution the residue of the pole at K_2 has to vanish, i.e.,

$$\lim_{K\to K_2}[(K-K_2)A(K,\omega)]=0. \tag{3.11}$$

Otherwise there would be a contribution $\sim e^{iK_2x}$ for $x\to+\infty$ giving rise to spatial growth and a divergence of $A(x\to+\infty,\omega)$ even for subcritical driving $\mu<0$. The physically motivated requirement that there is no growth $\sim e^{iK_2x}$ for $x\to+\infty$ is equivalent to selecting the ''retarded'' or causal Green function in the solution of the CGLE (cf. Appendixes A and B 1). Therein the solution is represented by a superposition of ''waves'' that propagate (in the frame comoving with velocity v) outwards, i.e., away from a localized perturbation source $\sim\delta(x-x_0)\delta(t-t_0)$ that creates a perturbation pulse at x_0, t_0. For $\mu<0$ the ''waves'' are damped while for $0<\mu<\mu_{\rm conv}^c$ they grow in the downstream direction within the frequency band (3.5). On the other hand, the ''advanced'' Green function describes inwards propagating waves $\sim e^{i[K_2(\omega)x-\omega t]}$ that create the pulse at x_0, t_0. They would cause even for $\mu<0$ a divergence of A at $x\to+\infty$.

Note that the requirement (3.11) implies that for a given forcing $f(x,\omega)$ the initial slope $\partial_x A(x,\omega)|_{x=0}$ of the amplitude at the inlet is fixed by the inlet value $A(x=0,\omega)$ and the forcing $f(K_2,\omega)=-i\int_0^\infty dx e^{-iK_2x}f(x,\omega)$. From Eqs. (3.10) and (3.11) one obtains the relation

$$i(\partial_x-iK_1)A(x,\omega)|_{x=0}+\frac{f(K_2,\omega)}{(1+ic_1)\xi_0^2}=0. \tag{3.12}$$

Using this restriction to eliminate the slope in Eq. (3.10) the physical solution of the CGLE can be written as the sum of two terms:

$$A(K,\omega)=A_{in}(K,\omega)+A_b(K,\omega). \tag{3.13a}$$

Here

$$A_{in}(K,\omega)=-\frac{A(x=0,\omega)}{K-K_1} \tag{3.13b}$$

is the contribution from the inlet fluctuations $A(x=0,\omega)$ while

$$A_b(K,\omega)=\frac{f(K,\omega)-f(K_2,\omega)}{(1+ic_1)\xi_0^2(K-K_1)(K-K_2)} \quad (3.13c)$$

is caused by bulk forcing. In real space the solution reads

$$A(x,\omega)=A_{in}(x,\omega)+A_b(x,\omega), \quad (3.14a)$$

where

$$A_{in}(x,\omega)=A(x=0,\omega)e^{iK_1x} \quad (3.14b)$$

and

$$A_b(x,\omega)=\frac{i}{(1+ic_1)\xi_0^2(K_1-K_2)} \times\left(\int_0^x dx'(e^{iK_1(x-x')}-e^{iK_2(x-x')})f(x',\omega) - (e^{iK_1x}-e^{iK_2x})\int_0^\infty dx' e^{-iK_2x'}f(x',\omega)\right). \quad (3.14c)$$

Note that the bulk part vanishes at the inlet boundary, $A_b(x=0,\omega)=0$.

B. Digression: constant bulk and inlet forcing

In this subsection we make a digression to investigate the special case

$$f(x,\omega)=2\pi\delta(\omega)f_0, \quad A(x=0,\omega)=2\pi\delta(\omega)A_0 \quad (3.15)$$

of constant (deterministic) forcing $f(x,t)=f_0$ in the bulk and constant inlet boundary condition $A(x=0,t)=A_0$. This investigation is useful and instructive for two reasons: (i) It allows one to check the general solution (3.14) for a special case that can easily be solved analytically in a direct way without Laplace transformation and that furthermore can easily be solved numerically. (ii) It gives insight into the way the initial slope $\partial_x A|_{x=0}$, inlet value A_0, and bulk forcing f_0 are tied to each other.

We consider in this subsection the stationary solution $A(x)$ of the CGLE, i.e., $A(x,\omega)=2\pi\delta(\omega)A(x)$. Then Eq. (3.14b) gives

$$A_{in}(x)=A_0e^{iK_1^0x} \quad (3.16a)$$

and (3.14c) becomes

$$A_b(x)=\frac{f_0}{(1+ic_1)\xi_0^2K_1^0K_2^0}(1-e^{iK_1^0x}) \quad (3.16b)$$

with $K_1^0=K_1(\omega=0)$ and $K_2^0=K_2(\omega=0)$ given by Eq. (3.3). The complete solution reads

$$A(x)=A_{in}(x)+A_b(x)=A_0e^{iK_1^0x}-\frac{f_0}{(1+ic_0)\mu}(1-e^{iK_1^0x}). \quad (3.16c)$$

Here we have used $(1+ic_1)\xi_0^2K_1^0K_2^0=-(1+ic_0)\mu$. The physically motivated restriction (3.11), (3.12) on the slope at the inlet becomes in our special case

$$\partial_xA(x)|_{x=0}=iK_1^0A_0-i\frac{f_0}{(1+ic_1)\xi_0^2K_2^0} =iK_1^0\left[A_0+\frac{f_0}{(1+ic_0)\mu}\right] \quad (3.17)$$

since $f(K_2,\omega)=-f_0 2\pi\delta(\omega)/K_2^0$ for constant forcing. We have checked the validity of Eq. (3.16c) also by direct numerical integration of the (nonlinear) CGLE.

C. Correlation functions

Here we investigate the frequency spectrum

$$C(x,\omega)=\int_{-\infty}^{\infty}d(t-t')e^{i\omega(t-t')}\,C(x,|t-t'|) \quad (3.18)$$

of the time-displaced autocorrelation function

$$C(x,|t-t'|)=\langle A(x,t)[A(x,t')]^*\rangle \quad (3.19)$$

of amplitude fluctuations $A(x,t)$ at the same downstream position x. Since the semi-infinite system with through-flow is spatially not translational invariant the correlations (3.19) depend explicitly on the position x. On the other hand, the statistical stationarity of the forcing processes in the bulk and at the inlet causes a temporal dependence only via $|t-t'|$. Using this property one has

$$C(x,\omega)=\frac{\langle A(x,\omega)[A(x,\omega')]^*\rangle}{2\pi\delta(\omega-\omega')}. \quad (3.20)$$

We consider inlet fluctuations $A(x=0,\omega)$ that are determined by forces operating outside the bulk fluid volume, for instance, by fluctuating forces in the upstream part of an experimental setup. Thus, in the convectively unstable regime the contribution $A_b(x,\omega)$ (3.14c) due to bulk forcing is uncorrelated with the inlet fluctuations $A(x=0,\omega)$ so that

$$\langle A(x=0,\omega)[A_b(x,\omega')]^*\rangle=0=\langle A_{in}(x,\omega)[A_b(x,\omega')]^*\rangle. \quad (3.21)$$

Therefore

$$C(x,\omega)=C_{in}(x,\omega)+C_b(x,\omega) \quad (3.22a)$$

is the sum of correlations

$$C_{in}(x,\omega)=e^{-2\,\mathrm{Im}K_1x}D(\omega) \quad (3.22b)$$

of the contribution $A_{in}(x,\omega)$ (3.14b) caused by inlet fluctuations and of correlations

$$C_b(x,\omega)=\frac{F}{2(1+c_1^2)\xi_0^4|K_1-K_2|^2}\left\{\frac{1}{\mathrm{Im}K_1}-\frac{1}{\mathrm{Im}K_2} +\left(4\,\mathrm{Im}\frac{1}{K_1^*-K_2}-\frac{1}{\mathrm{Im}K_1}-\frac{1}{\mathrm{Im}K_2}\right)e^{-2\,\mathrm{Im}K_1x} +4\,\mathrm{Re}\left[\left(\frac{1}{2\,\mathrm{Im}K_2}+\frac{i}{K_1^*-K_2}\right)e^{i(K_1-K_2)x}\right]\right\} \quad (3.22c)$$

of $A_b(x,\omega)$ (3.14c) caused by bulk forcing. Here

$$D(\omega)=C_{in}(x=0,\omega)=\frac{\langle A(x=0,\omega)[A(x=0,\omega')]^*\rangle}{2\pi\delta(\omega-\omega')} \tag{3.23}$$

is the fluctuation spectrum of the inlet amplitude. The expression (3.22c) for

$$C_b(x,\omega)=\frac{\langle A_b(x,\omega)[A_b(x,\omega')]^*\rangle}{2\pi\delta(\omega-\omega')} \tag{3.24}$$

is obtained directly from Eq. (3.14c) by using the force correlations

$$\langle f(x,\omega)[f(x',\omega')]^*\rangle=\delta(x-x')2\pi\delta(\omega-\omega')F. \tag{3.25}$$

Let us briefly discuss the small-x and the large-x behavior of $C(x,\omega)$: Since $C_b(x=0,\omega)=0$ one has $C(x=0,\omega)=C_{in}(x=0,\omega)=D(\omega)$. Furthermore, C_{in} varies linearly and C_b quadratically in x close to the inlet.

The large-x behavior is physically more interesting since it tells how and which frequency modes are amplified. Here one has to distinguish the two cases (i) $\mathrm{Im}K_1>0$ and (ii) $\mathrm{Im}K_1<0$. Case (i) holds for all ω if $\mu<0$ and for ω outside the band (ω_-,ω_+) of growing frequency modes if $\mu>0$. For these damped modes the autocorrelation approaches at large distances from the inlet the limit value

$$\lim_{x\to\infty}C(x,\omega)=\frac{F}{2(1+c_1^2)\xi_0^4|K_1-K_2|^2}\left(\frac{1}{\mathrm{Im}K_1}-\frac{1}{\mathrm{Im}K_2}\right). \tag{3.26a}$$

The fluctuations of these damped modes are influenced and sustained at large distances from the inlet only by the bulk forcing. The limiting value (3.26a) coincides with the autocorrelation

$$C_\infty(\omega)=\int_{-\infty}^{\infty}\frac{dk}{2\pi}\times\frac{F}{|(1+ic_1)\xi_0^2k^2-\mu(1+ic_0)-i(\omega-vk)\tau_0|^2} \tag{3.26b}$$

of amplitude fluctuations in an infinite system, $-\infty<x<\infty$, that is translational invariant without inlet boundary conditions.

In case (ii) of $\mathrm{Im}K_1<0$, i.e., for $\mu>0$ and $\omega_-<\omega<\omega_+$ there is exponential growth. Then the correlation function is dominated for large x by

$$C(x\to\infty,\omega)\to\left[D(\omega)-\frac{F}{2(1+c_1^2)\xi_0^4|K_1^*-K_2|^2}\times\left(\frac{1}{\mathrm{Im}K_1}+\frac{1}{\mathrm{Im}K_2}\right)\right]e^{-2\,\mathrm{Im}K_1x}. \tag{3.27}$$

To derive Eq. (3.27) from Eq. (3.22) we have used the relation

$$\frac{1}{|K_1-K_2|^2}\left(4\,\mathrm{Im}\frac{1}{K_1^*-K_2}-\frac{1}{\mathrm{Im}K_1}-\frac{1}{\mathrm{Im}K_2}\right)=\frac{-1}{|K_1^*-K_2|^2}\left(\frac{1}{\mathrm{Im}K_1}+\frac{1}{\mathrm{Im}K_2}\right). \tag{3.28}$$

Equations (3.22) for the spectra of amplitude fluctuations and their large-x limiting behavior are the central result of this paper. It allows one to assess the influence of (externally generated) inlet fluctuations and of bulk stochastic forces separately.

IV. INLET AND BULK GENERATED FLUCTUATIONS

Here we first introduce a simple model for the frequency spectrum $D(\omega)$ (3.23) of inlet fluctuations of the amplitude $A(x=0)$. It allows one to make quantitative estimates of the importance of their contributions $C_{in}(x,\omega)$ (3.22b) relative to those of the bulk generated fluctuations $C_b(x,\omega)$ (3.22c).

A. Model for inlet fluctuations

In Ref. [29] $D(\omega)$ was estimated by projecting transverse momentum current fluctuations in thermal equilibrium onto the critical mode of the hydrodynamic field equations. These fluctuations were assumed to be advected towards the inlet from an upstream part $x<0$ without deterministic driving, $\underline{\mu}=-1$, and to enter the main supercritical part of the experimental cell, e.g., via a porous plug at $x=0$. Thus, the Rayleigh number Ra or the Taylor number T in the upstream part was taken to be zero in [29]. In experiments, however, one often has an upstream section $-\underline{L}<x<0$ to the left of the inlet at $x=0$ in which the fluid is equilibrated at a finite subcritical driving $\underline{\mu}<0$. In the remainder of this paper we mark quantities characterizing such a subcritical upstream part of the system by an underbar.

Babcock, Ahlers, and Cannell [8] have numerically solved the stochastic CGLE for such a setup with $\underline{L}=0.1, \underline{\mu}=-0.1$, and boundary condition $A(x=-\underline{L},t)=0$. We consider a situation where $\underline{L}$ is sufficiently large. Then perturbations, e.g., from the pumping machinery that are swept at $x=-\underline{L}$ into the subcritical upstream part of the apparatus have decayed by the time the fluid reaches the inlet, $x=0$, of the supercritical part. Thus, one ideally has at $x=0$ only fluctuations in the hydrodynamic fields that are sustained by thermally activated fluctuating forces. The most important field fluctuations are those with wave numbers close to the critical one and with spatial variation in the directions perpendicular to the through-flow similar to the critical mode. We approximately describe the dynamics of the amplitude of these modes with the linear stochastic CGLE (2.7), now, however, for subcritical driving $\underline{\mu}<0$. Therein, the spectrum of amplitude fluctuations at $x=0$ that are generated at subcritical driving by thermal forcing $f(x\leqslant 0,t)$ alone—$\underline{L}$ is large—is given by Eq. (3.26) with $\mu=\underline{\mu}<0$:

$$D(\omega)=C_\infty(\omega;\underline{\mu})$$

$$=\frac{F}{2(1+c_1^2)\xi_0^4|\underline{K}_1-\underline{K}_2|^2}\left(\frac{1}{\mathrm{Im}\underline{K}_1}-\frac{1}{\mathrm{Im}\underline{K}_2}\right). \tag{4.1}$$

The total spectral power of these noise generated fluctuations of the amplitude $A(x=0)$ of the critical mode at the inlet

$$D(t=0)=\int_{-\infty}^{\infty}\frac{d\omega}{2\pi}D(\omega)=\frac{F}{4\tau_0\xi_0\sqrt{-\underline{\mu}}} \tag{4.2}$$

increases with increasing driving in the subcritical upstream section and diverges in the absence of nonlinearities in Eq. (2.7) at the critical driving $\underline{\mu}=0$. Thus, the estimate (4.1) is only realistic for a situation where the noise generated amplitudes in the upstream part are small enough to neglect the nonlinear contributions in the hydrodynamic field equations, i.e., for $\underline{\mu}$ not too close to zero. If that is the case then a variation $\propto 1/\sqrt{-\underline{\mu}}$ in the inlet contribution should be experimentally observable.

In Fig. 1 we show the inlet spectrum $D(\omega)$ (4.1) normalized by $\tau_0 D(t=0)$ versus reduced frequency $\omega\tau_0$ for several subcritical upstream control parameters as indicated. The inlet spectrum $D(\omega)$ is dominated by the term $1/\mathrm{Im}\underline{K}_1$. It controls the $\underline{\mu}$ variation of the peak height and of the peak width of $D(\omega)$ and it governs the strong enhancement of those modes around $\omega=0$ that can grow in the supercritical downstream part of the system.

Finally we would like to comment on the objection [25] against using, in a system without translational invariance, thermal equilibrium spectra for inlet fluctuations that come from the $\underline{\mu}=-1$ upstream part in [29]. This seems to be well justified in view of the fact that downstream forces do not influence upstream locations—downstream generated perturbations cannot propagate upstream if the through-flow is smaller than the convectively unstable threshold. Thus for

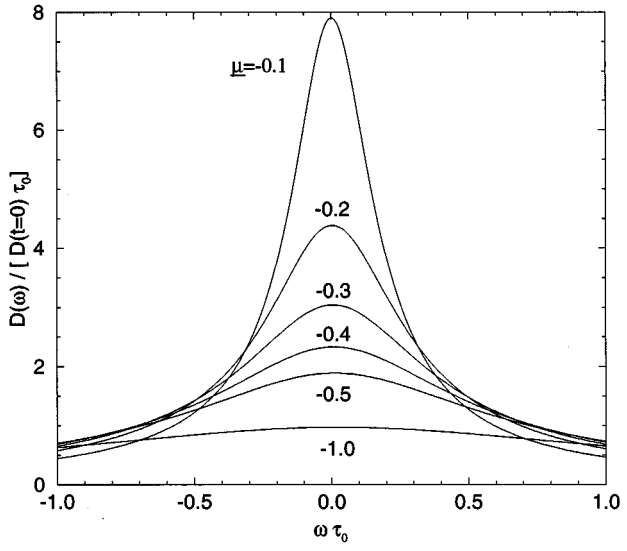

FIG. 1. Spectrum $D(\omega)$ (4.1) of amplitude fluctuations at the inlet normalized by $\tau_0 D(t=0)$ vs reduced frequency $\omega\tau_0$ for several $\underline{\mu}$. Parameters [39] are for Re=2.

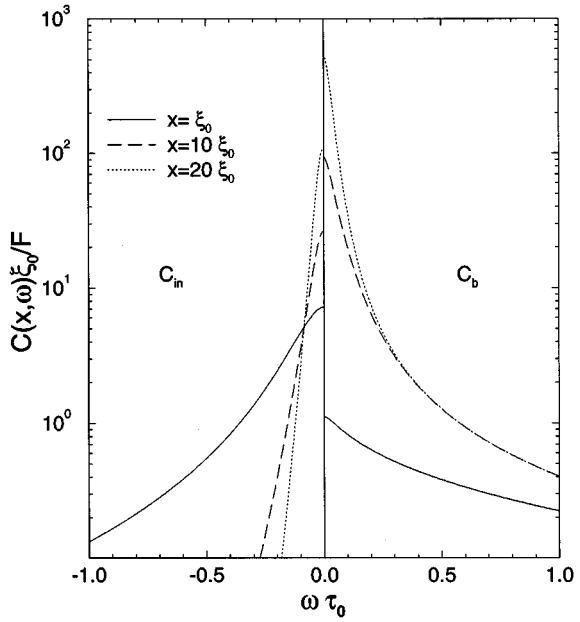

FIG. 2. Downstream evolution of the reduced contributions $C_{in}(x,\omega)$ (3.22b) and $C_b(x,\omega)$ (3.22c) to amplitude fluctuation spectra. Being practically symmetric in ω for our parameters $C_{in}\xi_0/F$ (left side) and $C_b\xi_0/F$ (right side) can be continued symmetrically to the other side. Inlet fluctuations $C_{in}(x=0,\omega)=D(\omega)$ are taken from our model with subcritical upstream driving $\underline{\mu}=-0.1$. Parameters [39] are Re=2, $\mu=\mu_{\mathrm{conv}}^c/2=0.03$.

any x in the upstream section that is sufficiently far away from $\underline{L}$ one should observe fluctuations as in an infinite system. For the stochastic CGLE this is reflected by the equality of Eqs. (3.26a) and (3.26b). But the corresponding property holds also for the full linear field equations with through-flow.

B. Comparison of inlet and bulk generated fluctuations

In Fig. 2 we show the downstream evolution of the spectral contributions $C_{in}(x,\omega)$ (3.22b) and $C_b(x,\omega)$ (3.22c) from inlet and bulk forcing, respectively, to the total spectrum of amplitude fluctuations. The contributions are reduced by F/ξ_0 measuring the forcing strength. The inlet fluctuations $C(x=0,\omega)=C_{in}(x=0,\omega)=D(\omega)$ are taken from the model of Sec. IV A with a subcritical upstream driving of $\underline{\mu}=-0.1$. The Reynolds number is Re=2 and the supercritical downstream driving is $\mu=\mu_{\mathrm{conv}}^c/2=0.03$. For these parameters the band limits (3.5) of amplification $\mathrm{Im}K_1(\omega)<0$ are $\omega_-\tau_0=-0.084$ and $\omega_+\tau_0=0.086$, respectively. While the logarithmic scale of the ordinate tends to obscure the boundaries between growing and decaying frequency modes the left border ω_- of the amplification band can be identified in the plots of $C_{in}(x,\omega)$ of Fig. 2 by their crossing point—there, C_{in} spectra at different x have the same value for $\mathrm{Im}K_1=0$.

The bulk contribution C_b that vanishes at the inlet is at a distance of one correlation length ξ_0 still smaller than the inlet contribution. Then, with a growing downstream dis-

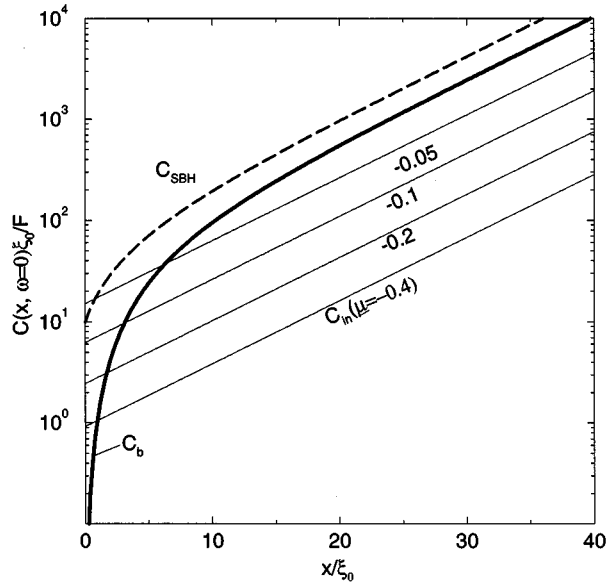

FIG. 3. Downstream growth of spectral peaks. They are located very close to $\omega=0$ for our parameters [39] Re=2, $\mu=\mu^c_{\rm conv}/2=0.03$. Thin lines show $C_{in}(x,\omega=0)\xi_0/F$ coming from inlet fluctuations (Sec. IV A) obtained for different subcritical upstream driving $\underline{\mu}$. For the SBH result $C_{\rm SBH}(x,\omega=0)\xi_0/F$ (B12) represented by the thick dashed line the inlet fluctuations are fixed by construction via μ,Re (cf. Appendix B 3).

tance C_b becomes larger. At $x=20\xi_0$ the bulk contribution has almost reached its large-x single exponential growth asymptotics $\propto e^{-2\,{\rm Im}K_1(\omega)x}$. There the contribution to C_b from the last term $\propto e^{i[K_1(\omega)-K_2(\omega)]x}$ in Eq. (3.22c) is already small.

That can also be seen in Fig. 3. There we show for the same supercritical downstream driving $\mu=\mu^c_{\rm conv}/2=0.03$ that was used in Fig. 2 the downstream growth of the spectral peak $C_b(x,\omega=0)$ in comparison with the peak height $C_{in}(x,\omega=0)$ of the inlet contribution—for our parameters the spectral maxima are located practically at $\omega=0$. C_{in} was evaluated for several subcritical upstream driving values of $\underline{\mu}$ as indicated. The dashed line labeled $C_{\rm SBH}$ is discussed in Appendix B3. Thus, for the values of $\underline{\mu}$ in Fig. 3 the bulk contribution rapidly outgrows the inlet contribution. A similar observation was made also in the numerical treatment of Babcock, Ahlers, and Cannell [8].

The slope of the straight lines C_{in} and of the asymptotics of C_b and $C_{\rm SBH}$ is given by $-2\,{\rm Im}K_1^0$, where the superscript 0 indicates that the eigenvalue K_1 is taken at $\omega=0$. In the far downstream region the ratio of the spectral maxima of C_b and C_{in} approaches according to Eq. (3.27) the limiting value

$$\lim_{x\to\infty}\frac{C_b(x,\omega=0)}{C_{in}(x,\omega=0)} = -\frac{F/D(\omega=0)}{2(1+c_1^2)\xi_0^4|K_1^{0*}-K_2^0|^2}\left(\frac{1}{{\rm Im}K_1^0}+\frac{1}{{\rm Im}K_2^0}\right). \tag{4.3}$$

If one uses for $D(\omega=0)$ the result (4.1) of our model one finds for the parameters of Fig. 3 that the bulk generated downstream fluctuations C_b dominate over the fluctuations that are swept into the system through the inlet whenever the upstream driving $\underline{\mu}<-0.025$. If the downstream driving μ is smaller than in the example of Fig. 3 then the size of inlet fluctuations that would ensure C_{in} to be comparable to C_b for large x would have to be larger—i.e., $\underline{\mu}$ would have to be even closer to zero.

Thus we conclude that *typically* the large- (small-) x behavior is governed by bulk (inlet) fluctuations. However, our upstream model clearly shows that in appropriately designed experimental upstream sections—with $\underline{L}$ being long enough to avoid influence of the pumping machinery operating at $x=-\underline{L}$—one can tune and enhance the inlet noise at $x=0$ almost arbitrarily by selecting the subcritical upstream driving $\underline{\mu}$ accordingly. Finally we would like to stress that our model for inlet fluctuations contains only internal thermal fluctuations generated in the subcritical upstream part. It does not contain other perturbations, e.g., from the pumping machinery, that might in an experimental setup be advected towards the inlet. Their contribution to the inlet fluctuation spectrum would have to be added to our model spectrum (4.1). However, since our general formulas in Sec. III have been derived for arbitrary inlet fluctuations with spectrum $D(\omega)$ they also apply to such a situation.

V. CONCLUSION

We have investigated the effect of inlet fluctuations and bulk stochastic forcing on noise sustained pattern growth in semi-infinite systems, $0\leqslant x$, with through-flow in the convectively unstable parameter regime. We have used a 1D CGLE that is appropriate for forward bifurcating structures in order to quantitatively compare both effects on the statistical dynamics of the downstream growth of the complex pattern amplitude $A(x,t)$.

To that end we have solved the linear stochastic CGLE subject to arbitrary, statistically stationary boundary conditions at the inlet $x=0$ in the presence of bulk additive forcing $f(x,t)$ with a spatial Laplace transform. This method is well suited for the semi-infinite geometry: inlet and bulk forcing are easily dealt with separately since they both appear explicitly and additively via boundary and inhomogeneous terms, respectively. Furthermore, this approach easily allows one to identify the contributions to the general mathematical solution from a pole at $K_2(\omega)$ in the complex wavenumber plane that have to be discarded on physical grounds since they would cause growth even for subcritical control parameters. The physically motivated restriction is equivalent to choosing the ''space-retarded, causal'' Green function that describes propagation away from (and not towards) a localized perturbation pulse. The restriction imposes a relation between the inlet conditions on A and $\partial_x A$ on the one hand and the bulk forcing f on the other hand. Thus, for example, the inlet derivative $\partial_x A$ is fixed in the physically relevant solution of the second-order (in space) CGLE by A at $x=0$ and the bulk forcing f.

We have investigated the effect of arbitrary statistically stationary inlet fluctuations that are independent from the bulk stochastic forces and that are, e.g., advected through the

inlet at $x=0$ into the system $x>0$ with the through-flow from an upstream subsystem, $x<0$. Then we have considered a simple model for such an upstream subsystem that contains thermal fluctuations only: it is held at some subcritical driving $\underline{\mu}<0$ and the thermally generated fluctuations that are advected towards the inlet are described by the stochastic CGLE. Thus, $\underline{\mu}$ allows one to tune the strength of the advected inlet fluctuation spectrum.

If the driving μ in the downstream part $x>0$ is subcritical then all frequency modes are damped. Then the correlation spectrum $C(x,\omega)$ of amplitude fluctuations is at large downstream distances from the inlet no longer influenced by the inlet fluctuations at $x=0$ and $C(x,\omega)$ approaches the translational invariant spectrum of an infinite system. However, for supercritical downstream driving $\mu>0$ inlet-forced as well as bulk-forced amplitude fluctuations are growing in the downstream direction for frequencies ω within a finite band. Typically the contribution $C_b(x,\omega)$ caused by the additive bulk forces to the correlation spectrum $C(x,\omega)$ of amplitude fluctuations at the downstream location x rapidly outgrows with increasing x the contribution $C_{in}(x,\omega)$ that follows from the upstream model for inlet fluctuations. In the large-x regime far from the inlet both contributions, $C_{in}(x,\omega)$ as well as $C_b(x,\omega)$, grow $\sim e^{-2\,\mathrm{Im}\,K_1(\omega)x}$ with $-\mathrm{Im}\,K_1>0$ having a maximum close to $\omega=0$. But the prefactors in C_b and C_{in} are such that there the amplitude fluctuation spectrum $C(x,\omega)$ is typically dominated by the bulk contribution $C_b(x,\omega)$. However, we have shown with our model how to realize experimental setups with subcritical upstream driving where the inlet fluctuations could be well controlled and well defined—uninfluenced by, e.g., the pumping machinery—and tuned to be large enough to dominate over the bulk part C_b.

Finally, a detailed comparison with a recent approach of SBH showed that the boundary condition that they use at the inlet implies fluctuations there that are strongly correlated with the bulk forcing. This enhances the amplitude fluctuations of the growing modes and thereby tends to overestimate the effect of thermal bulk forcing.

ACKNOWLEDGMENTS

This work was supported by the Go West program of the EC and by the DAAD. One of us (A.S.) acknowledges the hospitality of the Universität des Saarlandes. We thank A. Recktenwald and P. Büchel for help with the figures.

APPENDIX A: GREEN FUNCTION

We are interested in the Green function $G(x,x_0;t-t_0)$ of the CGLE as a solution of

$$[\tau_0(\partial_t+v\partial_x)-(1+ic_0)\mu-(1+ic_1)\xi_0^2\partial_x^2]G(x,x_0;t-t_0) = \delta(x-x_0)\,\delta(t-t_0) \tag{A1}$$

subject to an arbitrary boundary condition $G(x=0,x_0;t-t_0)$ at the inlet. Because of the semi-infinite geometry G depends on x and the location x_0 of the δ pulse separately. The temporal Fourier transform of G,

$$G(x,x_0;\omega)=\int_{-\infty}^{\infty} dt e^{i\omega(t-t_0)}G(x,x_0;t-t_0), \tag{A2}$$

is conveniently written as the sum of two contributions:

$$G(x,x_0;\omega)=e^{iK_1x}G(x=0,x_0;\omega)+\tilde{G}(x,x_0;\omega). \tag{A3}$$

Then the first term propagates the inlet condition in the downstream direction and the boundary condition on the bulk contribution

$$\tilde{G}(x,x_0;\omega)=\frac{i}{(1+ic_1)\xi_0^2(K_1-K_2)}[-e^{i(K_1x-K_2x_0)} + \theta(x-x_0)e^{iK_1(x-x_0)} + \theta(x_0-x)e^{iK_2(x-x_0)}] \tag{A4}$$

is $\tilde{G}(x=0,x_0;\omega)=0$. The physical solution (3.13) of the linear stochastic CGLE can then be written in the form

$$A(x,\omega)=\int_0^{\infty} dx_0 G(x,x_0;\omega)f(x_0,\omega) \tag{A5}$$

and

$$A(x,t)=\int_0^{\infty} dx_0 \int_{-\infty}^{t} dt_0 G(x,x_0;t-t_0)f(x_0,t_0). \tag{A6}$$

The x_0 integration covers the whole spatial domain $x_0\geqslant 0$. Causality implies contributions to come only from times $-\infty<t_0\leqslant t$ prior to the observation time t. The inlet condition on G is defined by the requirement that for any given $f(x_0,\omega)$ the integral

$$\int_0^{\infty} dx_0 G(x=0,x_0;\omega)f(x_0,\omega)=A(x=0,\omega) \tag{A7}$$

yields the *imposed* inlet condition $A(x=0,\omega)$ that can be chosen arbitrarily and in particular independent of f.

For the sake of comparison with the Green function G_{SBH} used by SBH (cf. Appendix B1) we mention that G [Eq. (A3)] can be rewritten as the following decomposition:

$$G(x,x_0;\omega)=e^{iK_1x}[G(x=0,x_0;\omega)-G_{\mathrm{SBH}}(-x_0;\omega)] + G_{\mathrm{SBH}}(x-x_0;\omega). \tag{A8}$$

Here

$$G_{\mathrm{SBH}}(x-x_0;\omega)=\frac{i}{(1+ic_1)\xi_0^2(K_1-K_2)}[\theta(x-x_0)e^{iK_1(x-x_0)} + \theta(x_0-x)e^{iK_2(x-x_0)}] \tag{A9}$$

is the Green function used by SBH and

$$G_{\mathrm{SBH}}(-x_0;\omega)=\frac{i}{(1+ic_1)\xi_0^2(K_1-K_2)}e^{-iK_2x_0} \tag{A10}$$

is its value at the inlet. Note that the ''space-retarded, causal'' nature of the Green function can readily be read off

from Eq. (A9). It describes spreading off—not contraction towards—the perturbation pulse at x_0: the first (second) exponential in Eq. (A9) accounts for the spreading in the downstream (upstream) direction with complex wave number K_1 (K_2). Downstream growth occurs for frequencies with $\mathrm{Im}K_1(\omega)<0$ while the spreading in the upstream direction is always damped given that $\mathrm{Im}K_2<0$.

Since the linear operator appearing in the CGLE (3.2), i.e., the square bracket in Eq. (A1), is $\propto(\partial_x - iK_1)\times(\partial_x - iK_2)$ it is clear from Eq. (A8) that both G and G_{SBH} solve Eq. (A1), however, with different inlet conditions.

APPENDIX B: COMPARISON WITH SBH

1. Green function $G_{\mathrm{SBH}}(x-x_0;\omega)$

Here we derive the expression (A9) for

$$G_{\mathrm{SBH}}(y;\omega)=\frac{i}{(1+ic_1)\xi_0^2(K_1-K_2)}\times[\theta(y)e^{iK_1y}+\theta(-y)e^{iK_2y}], \tag{B1}$$

with $y=x-x_0$ by temporally Fourier transforming the Green function

$$G_{\mathrm{SBH}}(y;\tau)=\frac{\theta(\tau)}{\tau_0}e^{(1+ic_0)\mu\tau/\tau_0}\times\int_{-\infty}^{\infty}\frac{dk}{2\pi}\exp\left[-(1+ic_1)\xi_0^2k^2\frac{\tau}{\tau_0}+ik(y-v\tau)\right] \tag{B2}$$

given in Eqs. (C18), (C19) of SBH for $\tau=t-t_0>0$. Inverting the sequence of integrations, one obtains

$$G_{\mathrm{SBH}}(y;\omega)=\frac{1}{\tau_0}\int_{-\infty}^{\infty}\frac{dk}{2\pi}e^{iky}\int_0^{\infty}d\tau\exp\left[i\omega\tau+(1+ic_0)\mu\frac{\tau}{\tau_0}-(1+ic_1)\xi_0^2k^2\frac{\tau}{\tau_0}-ikv\tau\right]$$
$$=\frac{1}{\tau_0}\int_{-\infty}^{\infty}\frac{dk}{2\pi}e^{iky}\int_0^{\infty}d\tau\exp\left[-(1+ic_1)\xi_0^2(k-K_1)(k-K_2)\frac{\tau}{\tau_0}\right]=\frac{1}{(1+ic_1)\xi_0^2}\int_{-\infty}^{\infty}\frac{dk}{2\pi}\frac{e^{iky}}{(k-K_1)(k-K_2)}. \tag{B3}$$

The above integral along the real k axis can be calculated as a contour integral in the complex k plane with the method of residues. For $y>0$ ($y<0$) one has to close the integration contour in the upper (lower) complex half plane.

The pole at K_2 contributes only for $y<0$ since it lies with $\mathrm{Im}K_2<0$ always in the lower half of the complex k plane. It yields the second term in Eq. (B1). The pole at K_1 lies for subcritical $\mu<0$ in the upper half of the complex k plane. It causes the term $\propto e^{iK_1y}$ for $y>0$ in Eq. (B1) to come from the contour closed in the upper half of the complex k plane. However, when $\mu>0$ this pole crosses the real k axis and moves into the lower k plane for frequencies within the band (3.5) of growing modes. In order to retain its contribution in Eq. (B1) for $y>0$ one has to deform the original integration path along the real k axis into a contour reaching into the lower k plane that encloses K_1 such that this pole remains in the interior.

Alternatively one can first perform the k integration in Eq. (B2) and then Fourier transform the result:

$$G_{\mathrm{SBH}}(y;\omega)=\frac{1}{2\xi_0\sqrt{(1+ic_1)\pi\tau_0}}\times\int_0^{\infty}\frac{d\tau}{\sqrt{\tau}}\exp\left[i\omega\tau+(1+ic_0)\mu\frac{\tau}{\tau_0}-\frac{(y-v\tau)^2\tau_0}{4(1+ic_1)\xi_0^2\tau}\right]. \tag{B4}$$

Using $\sqrt{\tau}$ as an integration variable one finds with Eq. (3.472-1) of Gradshteyn and Ryzhik [38] that

$$G_{\mathrm{SBH}}(y;\omega)=\frac{1}{\gamma}e^{\alpha y-\beta\sqrt{y^2}}, \tag{B5a}$$

with

$$\alpha=\frac{v\tau_0}{2(1+ic_1)\xi_0^2}, \tag{B5b}$$

$$\beta=\sqrt{\alpha^2-\frac{i\omega\tau_0+(1+ic_0)\mu}{(1+ic_1)\xi_0^2}}, \tag{B5c}$$

$$\gamma=2\beta(1+ic_1)\xi_0^2. \tag{B5d}$$

Expressing α, β, and γ in terms of the eigenvalues $K_{1,2}$ [Eq. (3.3)] and using the fact that $\sqrt{y^2}/y=\mathrm{sgn}(y)$ one verifies that Eq. (B5) agrees with Eq. (B1).

2. Amplitude fluctuations $A_{\mathrm{SBH}}(x,\omega)$

The amplitude fluctuations of SBH are expressed with the help of the Green function G_{SBH} as

$$A_{\mathrm{SBH}}(x,t)=\int_0^{\infty}dx_0\int_{-\infty}^{t}dt_0G_{\mathrm{SBH}}(x-x_0;t-t_0)f(x_0,t_0). \tag{B6}$$

Here we deal with the statistically stationary situation where the stochastic forces have been operating since the time $t_0=-\infty$. On the other hand, SBH enforce the initial condition $A_{\mathrm{SBH}}(x,t=0)=0$ at time $t=0$ by integrating in Eq. (B6) only from $t_0=0$ to $t_0=t$—cf. Eq. (C.20) in [25]. Since we are interested, however, in comparing the *long-time* properties of their results with ours this difference does not play a role—the formulas labeled with the subscript SBH in this and the next subsection refer to the long-time limit of the SBH results in [25].

In frequency space the long-time amplitude fluctuations of SBH follow with Eq. (B1) to be

$$A_{\mathrm{SBH}}(x,\omega)=\frac{i}{(1+ic_1)\xi_0^2(K_1-K_2)}\times\left[\int_0^x dx_0 e^{iK_1(x-x_0)}f(x_0,\omega)+\int_x^\infty dx_0 e^{iK_2(x-x_0)}f(x_0,\omega)\right]. \quad \text{(B7)}$$

Note that the SBH solution is a very special one in the sense that it assumes the long-time amplitude fluctuations at the inlet to be of the form

$$A_{\mathrm{SBH}}(x=0,\omega)=\frac{i}{(1+ic_1)\xi_0^2(K_1-K_2)}\times\int_0^\infty dx_0 e^{-iK_2x_0}f(x_0,\omega)=\frac{-f(K_2,\omega)}{(1+ic_1)\xi_0^2(K_1-K_2)}. \quad \text{(B8)}$$

Thus, the inlet boundary condition is not treated as an independent quantity that can be imposed on the solution of the CGLE. Rather the inlet boundary value for A is related to and determined explicitly by the bulk forcing $f(x_0,\omega)$. However, when we impose in our *general* solution (3.14) the special inlet condition $A_{\mathrm{SBH}}(x=0,\omega)$ of SBH we get the same result as SBH. In fact, our general solution (3.14) can be written in the form

$$A(x,\omega)=A_{\mathrm{SBH}}(x,\omega)+e^{iK_1x}[A(x=0,\omega)-A_{\mathrm{SBH}}(x=0,\omega)] \quad \text{(B9)}$$

with an inlet boundary condition $A(x=0,\omega)$ that is still free to be chosen.

Finally we mention that the derivative of the special SBH solution at the inlet,

$$\partial_x A_{\mathrm{SBH}}(x,\omega)|_{x=0}=\frac{-K_2}{(1+ic_1)\xi_0^2(K_1-K_2)}\times\int_0^\infty dx_0 e^{-iK_2x_0}f(x_0,\omega)=iK_2A_{\mathrm{SBH}}(x=0,\omega), \quad \text{(B10)}$$

is such that also the SBH solution obeys the relation (3.12),

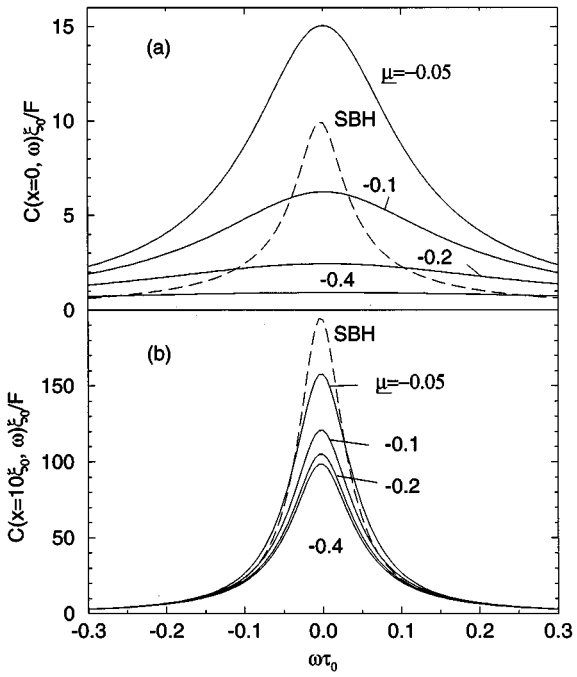

FIG. 4. Reduced correlation spectra of amplitude fluctuations at (a) inlet, $x=0$, and (b) further downstream, $x=10\xi_0$. Parameters [39] are Re=2, $\mu=\mu_{\mathrm{conv}}^c/2=0.03$. Full lines show our results using inlet fluctuation spectra (Sec. IV A) obtained for different subcritical upstream driving μ. Inlet fluctuations entering into the SBH result (dashed lines) are fixed by construction via μ,Re (cf. Appendix B 3).

$$i(\partial_x-iK_1)A_{\mathrm{SBH}}(x,\omega)|_{x=0}+\frac{f(K_2,\omega)}{(1+ic_1)\xi_0^2}=0, \quad \text{(B11)}$$

discussed in Sec. III A, which prevents unphysical behavior for $x\to\infty$.

3. Correlation function $C_{\mathrm{SBH}}(x,\omega)$

Using $\langle A_{\mathrm{SBH}}(x,\omega)[A_{\mathrm{SBH}}(x,\omega')]^*\rangle=2\pi\delta(\omega-\omega')C_{\mathrm{SBH}}(x,\omega)$ to evaluate the correlation spectrum one obtains from Eq. (B7)

$$C_{\mathrm{SBH}}(x,\omega)=\frac{F}{2(1+c_1^2)\xi_0^4|K_1-K_2|^2}\times\left[\frac{1}{\mathrm{Im}K_1}(1-e^{-2\,\mathrm{Im}K_1x})-\frac{1}{\mathrm{Im}K_2}\right] \quad \text{(B12)}$$

with inlet correlations being given by

$$C_{\mathrm{SBH}}(x=0,\omega)=\frac{F}{2(1+c_1^2)\xi_0^4|K_1-K_2|^2}\,\frac{-1}{\mathrm{Im}K_2}. \quad \text{(B13)}$$

These correlation spectra have to be compared with our result, Eqs. (3.22) and (3.23). Note that $F=2\xi_0\tau_0F_A^{\mathrm{SBH}}$ as mentioned already in Sec. II C.

To that end we show in Fig. 4 amplitude fluctuation spectra at the inlet, $x=0$, and further downstream, $x=10\xi_0$, for Re=2 and $\mu=\mu_{\mathrm{conv}}^c/2=0.03$. Full lines show our results us-

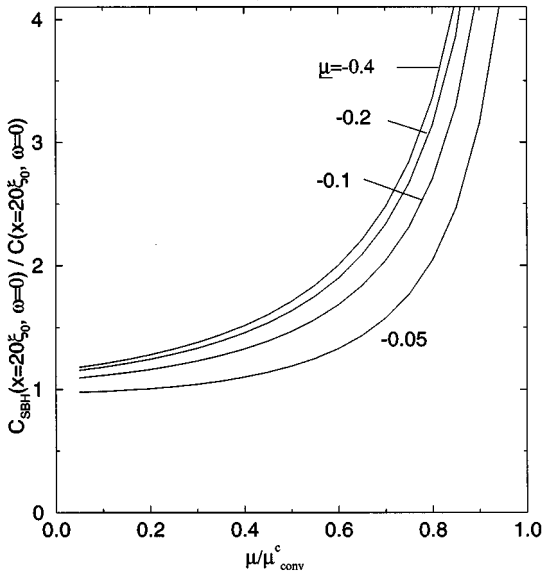

FIG. 5. Ratio of spectral peak heights of amplitude fluctuations according to SBH and to our work. The correlation spectra have almost reached their large-x asymptotic form at $x=20\xi_0$. Our spectra were evaluated using inlet fluctuations (Sec. IV A) obtained for different subcritical upstream driving $\underline{\mu}$. Inlet fluctuations entering into the SBH result are fixed by construction via μ,Re (cf. Appendix B 3). Parameters [39] are Re=2, $\mu=\mu^c_{\rm conv}/2=0.03$.

ing inlet fluctuation spectra (Sec. IV A) obtained for different subcritical upstream driving $\underline{\mu}$ as indicated. The most important difference is that in SBH the inlet fluctuations are determined by the bulk forcing f with a spectrum (B13) that is fixed by F, Re, and μ whereas in our more general case the inlet boundary condition on the amplitude A is still open. In the case that upstream fluctuations outside the main system generate our $A(x=0,\omega)$ the latter is statistically independent of amplitude fluctuations $A_b(x,\omega)$ (3.14c) that are generated in the bulk by the random forces f, i.e., $\langle A(x=0,\omega)[A_b(x,\omega')]^*\rangle=0$ (3.21).

This different correlation behavior influences not only the amplitude fluctuations close to the inlet but also the large-x correlation spectrum of the growing frequency modes with $\mathrm{Im}K_1<0$. Only the correlation spectra of the *damped* modes with $\mathrm{Im}K_1>0$ are in both approaches the same for large x: $C_{\rm SBH}(x\to\infty,\omega)=C(x\to\infty,\omega)=C_\infty(\omega)$. Equation (3.26) holds for the damped frequencies with $\mathrm{Im}K_1>0$ since at $x\to\infty$ these modes no longer feel any influence of the inlet boundary condition. However, for the *growing* modes with $\mathrm{Im}K_1<0$,

$$C_{\rm SBH}(x\to\infty,\omega)\to-\frac{F}{2(1+c_1^2)\xi_0^4|K_1-K_2|^2}\,\frac{1}{\mathrm{Im}K_1}\,e^{-2\,\mathrm{Im}K_1 x} \tag{B14}$$

differs from

$$C(x\to\infty,\omega)\to\left[D(\omega)-\frac{F}{2(1+c_1^2)\xi_0^4|K_1^*-K_2|^2}\times\left(\frac{1}{\mathrm{Im}K_1}+\frac{1}{\mathrm{Im}K_2}\right)\right]e^{-2\,\mathrm{Im}K_1 x}. \tag{B15}$$

Thus, if one just replaces in Eq. (B15) our inlet spectrum $D(\omega)$ by $C_{\rm SBH}(x=0,\omega)$ [Eq. (B13)] one does not recover the SBH result (B14) since the SBH spectrum was derived for inlet fluctuations $A_{\rm SBH}(x=0,\omega)$ [Eq. (B8)], which are correlated with the bulk forcing f while our inlet boundary condition on A is chosen to be externally determined and thus independent of the bulk forcing.

These additional correlations between inlet, $x=0$, and downstream positions, $x>0$, that are present in the SBH solution enhance the SBH spectra compared to our spectra. Consider, e.g., the case $\underline{\mu}=-0.05$ in Fig. 4 for which our inlet fluctuation spectrum is even larger than $C_{\rm SBH}(x=0,\omega)$. Nevertheless, the downstream amplitude fluctuation spectrum $C_{\rm SBH}(x,\omega)$ rapidly outgrows our $C(x,\omega)$. The effect of this correlation enhanced downstream growth of SBH can also be seen in Fig. 3—compare the dashed line for the peak height $C_{\rm SBH}(x,\omega=0)$ with our result $C(x,\omega=0)$ for $\underline{\mu}=-0.05$.

This effect can be measured quantitatively, e.g., by comparing the prefactors of the large-x exponential growth behavior of Eq. (B14) with that of Eq. (B15). To that end we ignore the imaginary coefficients c_0 and c_1 in view of their smallness [39]. Then the ratio of the spectral peak heights at $\omega=0$ has the form

$$\frac{C_{\rm SBH}(x\to\infty,\omega=0)}{C(x\to\infty,\omega=0)}\to\frac{\hat\mu}{2(1-\hat\mu)(1-\sqrt{1-\hat\mu})}\times\frac{\sqrt{1-\underline{\hat\mu}}}{\sqrt{1-\underline{\hat\mu}-\hat\mu/\underline{\hat\mu}}}, \tag{B16}$$

where

$$\hat\mu=\mu/\mu^c_{\rm conv}>0,\quad \underline{\hat\mu}=\underline{\mu}/\mu^c_{\rm conv}<0 \tag{B17}$$

denote reduced control parameters. For not too large $\hat\mu$ the ratio (B16) is close to 1. However, when $\hat\mu$ approaches 1 it becomes large. The coefficients c_0,c_1 remove the singularity present at $\hat\mu=1$ in Eq. (B16). In Fig. 5 the ratio $C_{\rm SBH}(x,\omega=0)/C(x,\omega=0)$ of the peak heights of the *full* correlation spectra is shown at $x=20\xi_0$ versus reduced downstream driving $\hat\mu$. This ratio differs only slightly from the large-x asymptote (B16) because of a small contribution from the last term in Eq. (3.22c).

The inlet fluctuations resulting from the upstream part of the system would have to be very large; i.e., $\underline{\mu}$ would have to be very close to zero in order to cause downstream fluctuation amplitudes that are as large as those of the SBH approach. Furthermore, if thermal equilibrium fluctuations were causing the inlet fluctuations as described by the unforced case $\underline{\mu}=-1$ in our upstream model the discrepancy would be even larger. Thus, in agreement with an assessment made in the introduction of [25] we conclude that the SBH result overestimates the effect of thermal noise mainly because the inlet boundary is not treated adequately.

[1] For a recent review see, e.g., M. C. Cross and P. C. Hohenberg, Rev. Mod. Phys. **65**, 851 (1993).
[2] For a review see, e.g., R. E. Kelly, Adv. Appl. Mech. **31**, 35 (1994).
[3] P. A. Monkewitz, Eur. J. Mech. B **9**, 395 (1990).
[4] H. W. Müller, M. Lücke, and M. Kamps, Europhys. Lett. **10**, 451 (1989).
[5] H. W. Müller, M. Lücke, and M. Kamps, Phys. Rev. A **45**, 3714 (1992).
[6] K. L. Babcock, G. Ahlers, and D. S. Cannell, Phys. Rev. Lett. **24**, 3388 (1991).
[7] K. L. Babcock, D. S. Cannell, and G. Ahlers, Physica D **61**, 40 (1992).
[8] K. L. Babcock, G. Ahlers, and D. S. Cannell, Phys. Rev. E **50**, 3670 (1994).
[9] A. Tsameret and V. Steinberg, Europhys. Lett. **14**, 331 (1991).
[10] A. Tsameret and V. Steinberg, Phys. Rev. E **49**, 4077 (1994).
[11] A. Tsameret and V. Steinberg, Phys. Rev. Lett. **67**, 3392 (1991).
[12] A. Tsameret, G. Goldner, and V. Steinberg, Phys. Rev. E **49**, 1309 (1994).
[13] P. Büchel, M. Lücke, D. Roth, and R. Schmitz, Phys. Rev. E **53**, 4764 (1996).
[14] D. Roth, P. Büchel, M. Lücke, H. W. Müller, M. Kamps, and R. Schmitz, Physica D **97**, 253 (1996).
[15] M. T. Ouazzani, J. K. Platten, H. W. Müller, and M. Lücke, Int. J. Heat Mass Transfer **38**, 875 (1995).
[16] R. J. Deissler and H. R. Brand, Phys. Lett. **130**, 293 (1988).
[17] W. Schöpf and I. Rehberg, Europhys. Lett. **17**, 321 (1992).
[18] I. Rehberg, S. Rasenat, M. la Torre-Juarez, W. Schöpf, F. Hörner, G. Ahlers, and H. R. Brand, Phys. Rev. Lett. **67**, 596 (1991).
[19] A. Bers, in *Basic Plasma Physics I*, edited by A. A. Galeev and R. N. Sudan (North-Holland, New York, 1983); R. J. Briggs, *Electron Stream Interaction with Plasmas* (MIT Press, Cambridge, MA, 1964).
[20] P. Huerre and P. A. Monkewitz, Annu. Rev. Fluid Mech. **22**, 473 (1990); J. Fluid Mech. **159**, 151 (1985); P. Huerre, in *Instabilities and Nonequilibrium Structures*, edited by E. Tirapegui and D. Villarroel (Reidel, Dordrecht, 1987), p. 141.
[21] R. J. Deissler, J. Stat. Phys. **40**, 371 (1985); **54**, 1459 (1989); Physica D **25**, 233 (1987); **18**, 467 (1986).
[22] R. Graham, Phys. Rev. A **10**, 1762 (1974); **45**, 4198(E) (1992); **18**, 467 (1986).
[23] P. C. Hohenberg and J. B. Swift, Phys. Rev. A **46**, 4773 (1992).
[24] W. Schöpf and W. Zimmermann, Phys. Rev. E **47**, 1739 (1993).
[25] J. B. Swift, K. L. Babcock, and P. C. Hohenberg, Physica A **204**, 625 (1994).
[26] M. Treiber, Phys. Rev. E **53**, 577 (1996).
[27] L. D. Landau and E. M. Lifshitz, *Statistical Physics* (Pergamon, London, 1958); *Fluid Mechanics* (Pergamon, London, 1959).
[28] R. J. Deissler, Phys. Rev. E **49**, R31 (1994).
[29] M. Lücke and A. Recktenwald, Europhys. Lett. **22**, 559 (1993).
[30] For a recent review see, e.g., R. Tagg, Nonl. Science Today **4**, 1 (1994).
[31] A. Recktenwald, M. Lücke, and H. W. Müller, Phys. Rev. E **48**, 4444 (1993).
[32] K. C. Chung and K. N. Astill, J. Fluid Mech. **81**, 641 (1977).
[33] D. J. Takeuchi and D. F. Jankowski, J. Fluid Mech. **102**, 101 (1981).
[34] A. Recktenwald, Diplom thesis, Universität des Saarlandes, 1991 (unpublished).
[35] R. Tagg, W. S. Edwards, and H. Swinney, Phys. Rev. A **42**, 831 (1990).
[36] A. Tsameret and V. Steinberg, Phys. Rev. E **49**, 1291 (1994).
[37] M. Dressler, Diplom thesis, Universität des Saarlandes, 1995 (unpublished); A. Recktenwald and M. Dressler (private communication).
[38] I. S. Gradshteyn and I. M. Ryzhik, *Table of Integrals, Series, and Products*, edited by Alan Jeffrey (Academic Press, New York, 1980).
[39] For the plots in this work we use CGLE parameters [34] that apply to the Rayleigh-Bénard system with Prandtl number 1 and through-flow:
$\mathrm{Ra}_c = 1707.74[1 + (\mathrm{Re}/35.9166)^2 + (\mathrm{Re}/65.1479)^4]$,
$k_c = 3.11633[1 + (\mathrm{Re}/176.783)^2 - (\mathrm{Re}/147.573)^4)]$,
$\omega_c = 3.64712\ \mathrm{Re}[1 + (\mathrm{Re}/213.8)^2]$,
$v = 1.229\ \mathrm{Re}[1 + (\mathrm{Re}/399)^2]$,
$\tau_0 = 0.07691[1 - (\mathrm{Re}/39.5)^2 + (\mathrm{Re}/42.9)^4]$,
$\xi_0^2 = 0.1480[1 - (\mathrm{Re}/38.5)^2 + (\mathrm{Re}/41.3)^4]$,
$c_0 = (\mathrm{Re}/141)[1 - (\mathrm{Re}/50.7)^2]$,
$c_1 = (\mathrm{Re}/40.0)[1 + (\mathrm{Re}/67.3)^2]$.